JCTC Journal of Chemical Theory and Computation

Diffusion of Hydrides in Palladium Nanoclusters. A Ring-Polymer Molecular Dynamics Study of Quantum Finite Size Effects

F. Calvo* and D. Costa†

Laboratoire de Spectrométrie Ionique et Moléculaire (LASIM), Université Claude Bernard Lyon 1 and Centre National de la Recherche Scientifique (CNRS) UMR 5579, Bát. A. Kastler, 43 Boulevard du 11 Novembre 1918, F69622 Villeurbanne, France

Received October 20, 2009

Abstract: The diffusion kinetics of hydrogen in bulk palladium and in Pd nanoclusters containing up to 512 atoms has been theoretically investigated at 3% loading using ring-polymer molecular dynamics simulations. The electronic ground-state energy surfaces are modeled using an explicit many-body potential fitted to reproduce the properties of bulk palladium and palladium hydrides. The diffusion constant, calculated by integration of the velocity autocorrelation function, shows Arrhenius behavior with inverse temperature. In addition, both the prefactor and activation energy are found to exhibit approximately linear variations with inverse cluster radius for sizes exceeding 128 Pd atoms. Vibrational delocalization generally enhances diffusion, this effect being stronger in clusters than in bulk. An inherent structure analysis from the positions of the centroids was used to characterize the diffusion mechanisms. Quantum effects lead to not only a higher coordination of hydrogen atoms both in bulk (fcc) palladium and in clusters but also favor further softening of the outer layers.

1. Introduction

Upon absorption of hydrogen, bulk palladium changes its mechanical and thermodynamical properties to a significant extent.[1−3] The two hydrides exhibited by this metal, namely the α phase at low concentration and the β phase at high concentration, should be considered as being similar to a solid solution and a defective NaCl rocksalt structure, respectively. They are separated from each other by a so-called miscibility gap associated with a phase transformation.[1] The amount of hydrogen that can be naturally absorbed is particularly high and reaches around 70% at saturation concentration,[1,4] which makes palladium a model system for hydrogen storage.[5] Palladium surfaces have interest of their own in the field of catalysis, with applications such as olefin hydrogenation or ammonia synthesis.[6] The catalytic efficiency of palladium can be magnified by further reducing the dimensionality and by studying clusters or nanoparticles, due to their higher surface/volume ratio. The higher sorption ability has been demonstrated by Huang and co-workers[7] for Pd nanoparticles smaller than 10 nm in diameter and supported on silica surfaces. More recently, Rather and co-workers[8] even found that an hyperstoichiometric concentration of 1.12 could be reached for surfactant-stabilized Pd nanoparticles of comparable sizes.

Nanometer palladium particles interacting with hydrogen have also been investigated for their structural and sorption properties.[9−15] Hydrogen-induced transitions between cubic and icosahedral clusters have been reported experimentally[10] and studied theoretically,[13] which could open some possible ways of controlling the nanoparticle shape by varying the external hydrogen pressure. The lattice expansion of Pd nanoparticles upon hydrogen absorption has been characterized by diffraction (X-ray and synchrotron radiation) techniques,[10,11,14] and one application to hydrogen sensor through tunneling has been proposed by van Lith and co-workers.[16] The interplay between the lattice size and the miscibility gap has been shown to depend on the presence

* Corresponding author. Telephone: 33 4 72 44 83 14. E-mail: fcalvo@lasim.univ-lyon1.fr.

† Present address: Groupe Métallurgie, MMC, EDF, Les Renardières, F-77818 Moret-sur-Loing, France.

10.1021/ct900554r
Published on Web 01/13/2010

of encapsulating surfactant molecules.[12,14] Very recently, Di Vece and co-workers[15] found that hydrogen adsorption can lead to Ostwald ripening of a film assembly of Pd nanoparticles at room temperature. These last examples further emphasize the important role of the surface on the hydrogenation process.

The mechanism for hydrogen diffusion in bulk palladium has been identified as a hopping motion between octahedral sites through intermediate tetrahedral sites,[17,18] and the variations of the diffusion constant $D(T)$ generally show Arrhenius behavior with inverse temperature:

$$D(T) \simeq D_0 \exp\left[-\frac{A}{k_B T}\right] \quad (1)$$

where the prefactor D_0 accounts for a typical attempt frequency, and A is an activation energy. The Arrhenius behavior also holds for deuterium, despite this isotope is known to occupy preferentially tetrahedral sites due to less favorable zero-point energy correction.[18−20] Most theoretical works aimed at characterizing the diffusion constant have so far relied on harmonic transition-state theory (TST),[21,22] which explicitly employs such an Arrhenius form. This approach, together with conflicting experimental measurements, has been criticized in the recent review by Jewell and Davis.[23] The static TST seems justified by the complexity of the overall diffusion process, since it can operate using accurate energetics obtained with methods that explicitly account for electronic structure and includes quantum tunneling effects using dedicated models.[24,25] Harmonic TST is also useful for studying hydrogen diffusion on free Pd surfaces[26,27] but cannot deal in itself with nonperiodic systems, such as nanoparticles. One extension of TST, recently applied by Hao and Sholl[28] to diffusion in amorphous Fe_3B, consists of sampling local minima connected by transition states and performing a kinetic Monte Carlo simulation of the hydrogen diffusion process. This approach allows multiple hydrogen atoms to be dealt with simultaneously and can also be carried out at first-principle levels using modern molecular dynamics techniques. However, it still neglects the motion of palladium atoms, which may be particularly important near the free surfaces of nanoparticles.

Diffusion constants for hydrogen motion in fcc palladium have also been calculated by direct molecular dynamics simulations by various authors,[17,29,30] who used explicit potentials. The molecular dynamics approach treats hydrogen atoms as classical particles because a full quantum treatment is practically unfeasible for this problem. Wavepacket simulations could be performed for H_2 molecules interacting with free Pd surfaces,[31,32] but this method is limited to very few degrees of freedom and, in particular, also assumes host Pd atoms to remain fixed. Semiclassical techniques, such as those based on the path-integral representation of quantum mechanics,[33] are a powerful alternative which can address the aforementioned limitations. Classical and quantum Monte Carlo simulations have been performed by Chen and coworkers,[34] who investigated the stable structures, the adsorption sites, and the temperature effects in small Pd−H clusters. Path-integral methods have also been used by Forsythe and Makri to study diffusion of hydrogen and deuterium in crystalline silicon.[35]

In the present work, the diffusion of hydrogen in palladium has been investigated using quantum ring-polymer molecular dynamics (RPMD).[36] The RPMD method provides exact results for the quantum dynamics in the limit of harmonic systems or in short time scales[38] and is accurate for the velocity autocorrelation function up to a leading error of $\mathcal{O}(t^6)$, which is better than the corresponding error of the centroid molecular dynamics of Cao and Voth[37] that scales as $\mathcal{O}(t^4)$. Since its introduction, the RPMD method has been applied to several quantum diffusion processes,[39,40] particularly for the similar problem of hydrogen impurities in condensed water,[41] and we use it here for both fcc palladium and Pd nanoparticles. Our main motivation is to characterize the extent of finite size effects on the diffusion constant of hydrogen in palladium, following our previous investigations on the structural and dynamical properties of Pd−H clusters.[13,42] Our main result is that, similar to bulk palladium, the diffusion of hydrogen in Pd nanoclusters follows Arrhenius behavior but with prefactors and activation energies that strongly depend on the number of Pd atoms. Above some size, both quantities are found to vary approximately linearly with inverse cluster radius, a well-known manifestation of cluster size effects in the scaling regime.[43]

The article is organized as follows: In Section II, we briefly review the potential energy surface chosen to model the interaction among Pd and H atoms and give some details about our implementation of the RPMD method for the present systems. The results on the diffusion constants are given and discussed in Section III, where scaling laws relating the Arrhenius parameters to the cluster size are proposed. In this section, we also attempt to analyze the role of quantum vibrational effects on the diffusion mechanisms by looking at the instantaneous inherent structures, thus getting insight into the nature of adsorption sites in both bulk and finite Pd systems. A summary and some perspectives finally end the paper in Section IV.

II. Methods

Our computational study relies on the recently introduced ring-polymer molecular dynamics technique.[36] Because the systems we deal with are rather large (up to several hundreds of atoms), we could not afford an explicit description of the electronic structure of palladium hydrides and turned instead to semiempirical many-body potentials. Several groups have employed models of similar complexity in previous work on Pd−H systems in both bulk[17,29,30,44] and nanoscale[9,13,34,42,45] forms.

A. Potential. The many-body alloy (MBA) model of Zhong and co-workers[46] served as a template for the present investigation. This potential is based on the second moment approximation to the electronic density of states in the tight-binding model and expresses the cohesion energy of the N-atom system with configuration $\mathbf{R} = \{x_i, y_i, z_i\}$ as

$$V(\mathbf{R}) = \sum_{i<j} \varepsilon_{ij} \exp\left[-p_{ij}\left(\frac{r_{ij}}{r_{ij}^0} - 1\right)\right] - \sum_i \left\{ \sum_{j \neq i} \zeta_{ij}^2 \exp\left[-2q_{ij}\left(\frac{r_{ij}}{r_{ij}^0} - 1\right)\right]\right\}^{1/2} \quad (2)$$

where ε, ζ, p, q, and r^0 are 3×5 parameters defined for all pairs of elements Pd−Pd, H−H, and Pd−H. These parameters were originally optimized to reproduce mechanical properties of bulk palladium hydrides and of some energetic properties of H and H_2 adsorbed on ⟨001⟩ and ⟨110⟩ Pd surfaces, all computed using density functional theory (DFT) within the local density approximation.[46] As shown in a previous contribution,[13] this original potential does not perform so well for hydrides absorbed in fcc palladium, at least when compared with more sophisticated recent calculations.[22] A much better agreement could be reached simply by borrowing the Pd−Pd parameters from another work by Rey and co-workers,[47] employing a similar expression as eq 2 but for pure palladium. The new set of combined parameters are given in Table I.

The new potential predicts the correct lattice size (3.89 Å) and the cohesion energy (3.91 eV/atom) for pure fcc palladium at 0 K. The most significant improvement over the initial MBA model of Zhong et al. lies in the binding energy of hydrogen in fcc palladium, which changes from −0.79 to −0.15 eV with the new parameters (octahedral site), after taking zero-point energy corrections into account at the harmonic level.[13] The latter value is in good agreement with the DFT result (GGA level) of −0.16 eV obtained by Kamakoti and Sholl.[22]

The above potential was first used to locate relevant structures for the Pd−H clusters to be used subsequently as initial configurations for the molecular dynamics trajectories. Global optimization by Monte Carlo plus by minimization was carried out, starting with large icosahedral clusters of pure palladium and inserting several hydrogen atoms at random locations before locally optimizing the geometry. In the present work, a fixed low hydrogen concentration of 3% was kept for a better comparison with available data.[17] Our bulk reference system is $Pd_{256}H_8$, which was treated using periodic boundary conditions in the minimum image convention and without truncating the interactions. Cubic boxes of volume $V = L^3$ were taken to depend on temperature in order to mimic the thermal expansion naturally occurring in experimental palladium hydride under fixed pressure. We chose the same linear dependence for the lattice spacing $a(T)$ as the authors of ref 17 for the same system, namely $a(T) = a(0)[1 + \alpha T]$, with $a(0) = 3.89$ Å and $\alpha = 2.1 \times 10^{-5}$ K^{-1} in the temperature range 500−1 000 K. This expression for $a(T)$, which accounts reasonably well for the measured expansion of the Pd lattice upon absorbing low amounts of hydrogen,[2] gives the $Pd_{256}H_8$ system a box length of $L(T) \approx L(0)[1 + \alpha T]$ with $L(0) = 8.300$ Å. In our simulations of the bulk system, the hydrogen atoms were initially placed in octahedral sites distant from each other (see Figure 1) for both quantum and classical simulations.

In order to unravel size effects in nanoscale Pd−H systems, the clusters were chosen at the same hydrogen concentration as the bulk, and we studied $Pd_{64}H_2$, $Pd_{128}H_4$, $Pd_{256}H_8$, and $Pd_{512}H_{16}$ without imposing periodic boundaries. Our search for stable structures consisted of 10^3 basin-hopping moves, which lead to icosahedral shape with subsurface absorbed hydrogens, two examples of which are shown in Figure 1. While our global optimization was rather limited, the structures obtained only served as initial configurations for the molecular dynamics trajectories, which were conducted at significantly high temperatures $T \geq 400$ K in order to detect some diffusion under the relatively short simulated times. Under these conditions, the global minimum structure is not so relevant, especially since many isomers differing in the hydrogen sites have comparable energies.[13]

Table I. Parameters of the Many-Body Potential Defined by eq 2, as Used in This Work[a]

pair type	ε (eV)	ζ (eV)	p	q	r^0 (Å)
Pd−Pd	0.17375	1.70769	10.8874	3.75433	2.748
H−H	0.1601	0.9093	5.28	3.22	2.3
Pd−H	0.6794	2.5831	5.5	2.2	1.769

[a] The Pd−Pd parameters are taken from ref 47, while Pd−H and H−H parameters are those proposed by Zhong et al. (ref 46).

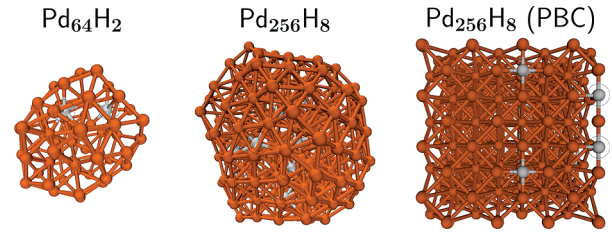

Figure 1. (Color online) Stable configurations used for the initial conditions of the simulations. Left: $Pd_{64}H_2$ cluster; middle: $Pd_{256}H_8$ cluster; and right: $Pd_{256}H_8$ with fcc lattice and with periodic boundary conditions (PBC). Some hydrogen atoms are highlighted with black circles.

B. Ring-Polymer Molecular Dynamics. The diffusion kinetics of hydrogen in Pd was studied using molecular dynamics simulations. Quantum vibrational effects were included with the ring-polymer molecular dynamics method developed by Craig and Manolopoulos.[36] It is not the purpose of the present paper to review this method in detail or how it compares with the related centroid molecular dynamics technique of Cao and Voth,[37] so we will only briefly describe its main features of relevance to the present problem.

RPMD is based on the so-called primitive path-integral representation of the quantum partition function. In the RPMD method, each classical atom is described by a number M of "beads" or monomers that act as imaginary time slices along the thermal path. These monomers interact successively through effective harmonic bonds, in such a way that the dynamics of the system is ruled by the following Hamiltonian:[36]

$$H(\{\mathbf{R}_i, \mathbf{P}_i\}) = \sum_{i=1}^{M} \sum_{\alpha \in \text{atoms}} \frac{\vec{p}_{i,\alpha}^2}{2m_{i,\alpha}} + \sum_{i=1}^{M} \sum_{\alpha \in \text{atoms}} \frac{m_{i,\alpha} M}{2\beta^2 \hbar^2} \|\vec{r}_{i,\alpha} - \vec{r}_{i+1,\alpha}\|^2 + \frac{1}{M} \sum_{i=1}^{M} V(\mathbf{R}_i) \quad (3)$$

In the previous equation, we have denoted $\mathbf{R}_i$ and $\mathbf{P}_i$ as the set of positions and the associated momenta of atoms that belong

to the replica i, $1 \le i \le M$. The vector $\vec{r}_{i,\alpha}$ and associated momentum $\vec{p}_{i,\alpha}$ refer to atom α among replica i. In eq 3, we have implicitly used the cyclic condition $\vec{r}_{M+1,\alpha} = \vec{r}_{1,\alpha}$ for all α. In RPMD, the atomic mass $m_{i,\alpha}$ is taken just as the physical mass m_α, which is the main practical difference with the partially adiabatic version of the centroid molecular dynamics method.[36,48]

Solving the equations of motion for the above Hamiltonian was shown by Craig and Manolopoulos to yield correct quantum dynamics for the centroids $\bar{\mathbf{R}} = \{\bar{\mathbf{r}}_\alpha\}$:

$$\bar{\mathbf{r}}_\alpha(t) = \frac{1}{M}\sum_{i=1}^{M} \vec{r}_{i,\alpha} \tag{4}$$

in the $t \to 0$ and harmonic $V(\mathbf{R})$ limits.[36,38] In practice, the equations are solved in the normal mode representation, which diagonalizes the harmonic part of eq 3. We denote $\mathbf{K}$ as the matrix with elements $\mathbf{K}_{ij} = 2\delta_{ij} - \delta_{i,j-1} - \delta_{i,j+1}$ (and the cyclic condition) as well as the unitary eigenvector matrix $\mathbf{U}$, which diagonalizes $\mathbf{K}$ as $\mathbf{U}^T\mathbf{K}\mathbf{U} = \mathrm{diag}(\lambda_i)$, λ_i being the corresponding eigenvalues. Under the linear transformation from the Cartesian coordinates $\{\vec{r}_{i,\alpha}\}$ to the normal modes $\{\vec{a}_{k,\alpha}\}$:

$$\vec{a}_{k,\alpha} = \frac{1}{\sqrt{M}}\sum_{i=1}^{M} U_{ki}\vec{r}_{i,\alpha} \tag{5}$$

the Hamiltonian becomes decoupled

$$\begin{aligned} H(\{\mathbf{A}_k, \mathbf{\Pi}_k\}) &= \sum_{k=1}^{M}\sum_{\alpha\in\text{atoms}} \frac{\vec{\pi}_{k,\alpha}^2}{2m_\alpha} \\ &+ \sum_{k=1}^{M}\sum_{\alpha\in\text{atoms}} \frac{m_\alpha M}{2\beta^2\hbar^2}\lambda_k \vec{a}_{k,\alpha}^2 \\ &+ \frac{1}{M}\sum_{i=1}^{M} V\left(\left\{\sqrt{M}\sum_{k=1}^{M} U_{ik}\vec{a}_{k,\alpha}\right\}\right) \end{aligned} \tag{6}$$

where we have denoted $\vec{\pi}_{k,\alpha} = m_\alpha\sqrt{M}\mathrm{d}\vec{a}_{k,\alpha}/\mathrm{d}t$ as the momentum of atom α among replica k. This normal mode expression is especially useful for propagating the equations of motion because the decoupling of harmonic bonds allows their analytical integration using the reference system propagation algorithm,[49] hence, no loss in time step duration with respect to the classical case $M = 1$.

An important issue of path-integral molecular dynamics, especially relevant when simulating finite-size systems, relates to thermostating. The effective potential of eqs 3 and 6 explicitly depends on some inverse temperature β, however, the RPMD dynamics is Newtonian. To address these difficulties, Craig and Manolopoulos originally advocated that the atomic momenta be periodically redrawn from the Maxwell−Boltzmann distribution.[36] In the present work, we have followed a different strategy by coupling each normal mode vector $\vec{a}_{k,\alpha}$, carrying 3 degrees of freedom, to a separate Nosé-Hoover thermostat. This simulation is only carried out to generate proper initial conditions pertaining to the canonical ensemble at a fixed temperature, from which the Hamilton equations of motion of the RPMD method are solved without coupling with the thermostat.[50] In the case of finite systems, the angular momentum of the centroids motion is not conserved during the thermostated equilibration stage, which may result in some undesired global rotation of the system during the subsequent RPMD propagation. This rotation can be suppressed by adding some extra angular velocity that exactly compensates the current angular momentum, a method recently used by Witt and co-workers.[51]

Diffusion processes have been characterized by evaluating the Kubo-transformed position and the velocity autocorrelation functions and by monitoring the mean square displacement of the centroids and the diffusion coefficient D. Within the RPMD framework, and neglecting exchange effects, the quantum mechanical expression for D is approximated by the Green−Kubo relation[39,40] involving the centroids velocities:

$$D \simeq \frac{1}{3}\int_0^\infty \langle \bar{\mathbf{v}}(t)\times\bar{\mathbf{v}}(0)\rangle \mathrm{d}t \tag{7}$$

where the average is taken over the different hydrogen atoms and multiple time origins, $\bar{\mathbf{v}}(t)$ being expressed for atom α as

$$\bar{\mathbf{v}}_\alpha(t) = \frac{1}{M}\sum_{i=1}^{M}\frac{\vec{p}_{i,\alpha}}{m_\alpha} \tag{8}$$

Likewise, the mean square displacement $\langle \bar{r}^2\rangle(t)$ is approximated from the centroids position $\bar{\mathbf{r}}_\alpha$, eq 4, which is also obtained from the normal mode $\vec{a}_{k,\alpha}$ corresponding to $\lambda_k = 1$. This centroid approximation reverts to the common classical expressions in the case of $M = 1$ and is exact in the limit of short times or harmonic potentials.[36,38]

For bulk systems, the calculated diffusion constant is known to depend on the size of the simulation box, and several authors[52,53] have shown that the asymptotic (infinitely large box) diffusion constant should include a hydrodynamic finite box correction proportional to $k_B T/\eta L$, where η is the viscosity. We have not tried to calculate the parameter η from simulations, but due to these corrections, the values for the diffusion constants of all bulk samples should be meant as lower bounds.

The hydrodynamic corrections for the bulk system are due to the spurious interactions between particles and their periodic images, thus, they do not have a counterpart in clusters. However, and strictly speaking, the diffusion constant should be zero for any finite system at any temperature because the mean square displacement cannot grow arbitrarily large in a restricted volume. The same problem arises for confined solvated systems, and Berne and co-workers have proposed methods based on fluctuating boundary conditions to deal with such situations.[54,55] Following Beck and Marchioro,[56] the time scale for calculating the velocity autocorrelation function was chosen sufficiently long with respect to the vibrational period but not exceedingly long, in order to avoid the saturation regime of the mean square displacement.

C. Numerical Details. The simulations for the periodic systems have been performed in the 500−1 000 K temperature range by 100 K steps and for all clusters in the 400−600 K range by 50 K steps. The first thermalization stage was carried out with thermostated RPMD trajectories

employing a short time step of 0.05 fs, for a duration of 2×10^5 steps (10 ps). The number of beads was taken either as $M = 1$ (classical case) or $M = 24$ to account for quantum delocalization. Intermediate values were tried also to assess the convergence at this higher value (see below). From the last 5 ps of the canonical simulations, 100 initial conditions were saved every 50 fs for further propagation without the thermostats. Each RPMD trajectory was then carried out for 20 ps with time step of 0.2 fs. Along these trajectories, the mean square displacement of centroid positions and the velocity autocorrelation functions were accumulated over 10 ps long time windows before final averaging over all trajectories.

In the case of clusters, these various MD trajectories sometimes had to be repeated, especially at high temperatures due to the spontaneous desorption of H_2 molecules into vacuum. Such dissociation events turned out to take place even more often for quantum simulations but would have hindered the calculation of the diffusion constant by contributing dominantly to the autocorrelation functions.

In addition to diffusion observables, we monitored the atomistic mechanisms of diffusion by periodically quenching the system to either its nearest classical local minimum or its inherent structure. Starting from the centroids positions $\bar{\mathbf{R}} = \{\bar{\mathbf{r}}_\alpha\}$, the potential energy V was locally minimized by a conjugate gradient. The set of structures obtained with this scanning procedure were eventually analyzed in terms of hydrogen coordination inside palladium sites.

III. Results

We first consider the influence of the Trotter number M on the centroids trajectories in the case of the periodic system $Pd_{256}H_8$ at intermediate temperature $T = 800$ K. The optimal value for M should depend first on the system as well as on the temperature, more beads being required to describe the increasingly broad nuclear wave functions as T decreases. We were not able to carry out reliably converged simulations for the largest 528-atom cluster with $M > 24$ due to the frequent hydrogen desorptions at temperatures $T \geq 500$ K that required restarting the trajectories.[57]

The time variations of the mean square displacement of hydrogen atoms are represented in Figure 2 for different values of M ranging from 1 to 24. At the temperature considered here, hydrogen exhibits some clear diffusion manifested on the positive slope of $\langle \bar{r}^2 \rangle(t)$ for times longer than about 3 ps. The classical and quantum mean square displacements show different behaviors, with the classical motion slightly less diffusive by about 16%. However, looking at the diffusion constants obtained from the integrated velocity autocorrelation function, this factor reduces to 14% for $M = 16$, instead of 24, and to 9% for $M = 8$. The discrepancy between the results obtained for $M = 16$ and $M = 24$ is rather small. Additional simulations for the smallest system $Pd_{64}H_2$ at 400 K using $M = 48$ indicate a further increase of the diffusion rate with respect to the $M = 24$ results, however, the effect is marginal and lies below 2%. Based on these observations and keeping computational feasibility into account, we believe that the error associated with employing the fixed value of $M = 24$ for the Trotter discretization number in our simulations should not exceed 5% in the estimated diffusion constants.

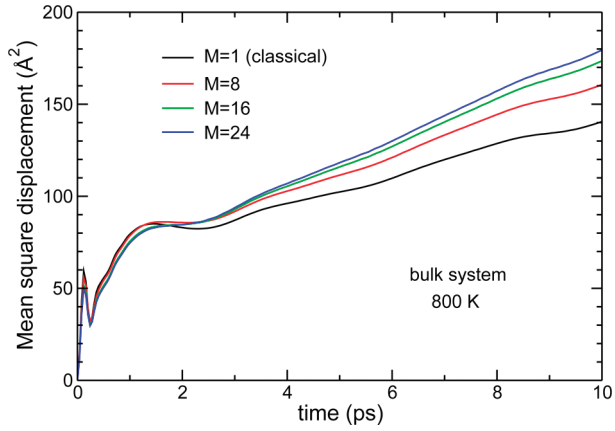

Figure 2. Mean square displacement of hydrogen atoms in Pd_{256} with periodic boundary conditions, as a function of time for different numbers of beads M in the RPMD simulations. The temperature is 800 K.

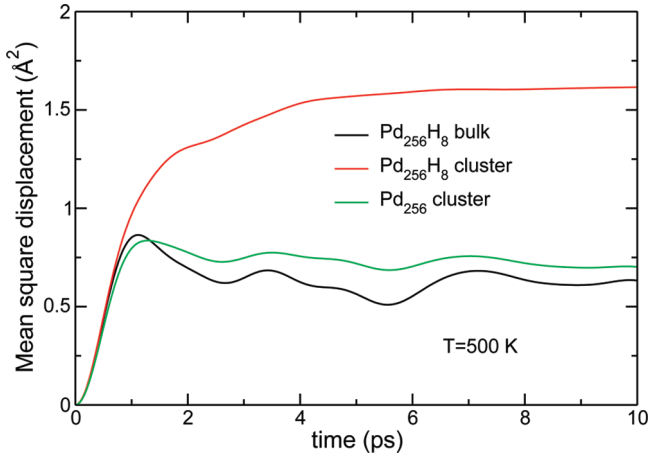

Figure 3. Mean square displacement of palladium atoms in several systems, as a function of time, as obtained from the simulations at 500 K. Classical molecular dynamics were used for the pure Pd cluster.

Hydrogen absorbed in bulk palladium is known to alter its thermomechanical properties,[1−3] and we have investigated the palladium motion in both periodic and finite systems. Figure 3 shows the mean square displacement of Pd atoms for the bare and hydrogenated 256-atom systems, as a function of time and temperature at $T = 500$ K. At this temperature, the bare palladium cluster is essentially solid-like,[13] and the atoms vibrate around their equilibrium positions. The dynamics of bulk palladium hydride is also poorly diffusive as far as the Pd atoms are concerned. In contrast, Pd atoms in the free $Pd_{256}H_8$ cluster remarkably exhibit some diffusion. The variations of the atom-resolved displacement indices, together with direct visual inspection, indicate that the cluster is softer near the hydrides and is even partially melted at the surface. This agrees with our previous findings in classical Pd−H nanoclusters[13] and is also consistent with previous studies by Grönbeck and co-workers, who performed classical molecular dynamics simulations with the original MBA potential.[45] The melted surface and the relatively more rigid core result from some

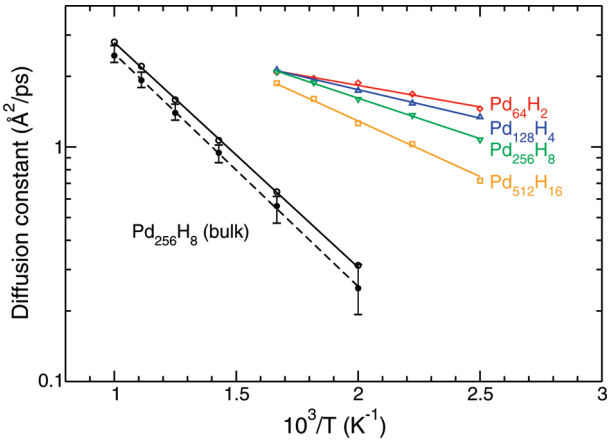

Figure 4. Diffusion constant of hydrogen atoms in bulk and finite palladium systems, as obtained from classical (solid circles) or quantum (open symbols) simulations. The straight lines are Arrhenius fits.

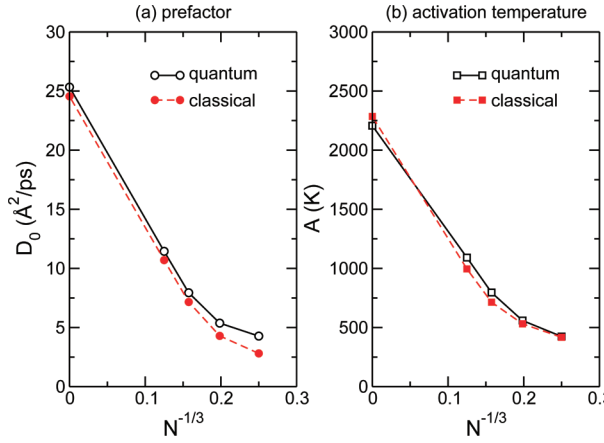

Figure 5. Variations of Arrhenius parameters with inverse cluster size, as obtained from classical and RPMD simulations: (a) Arrhenius prefactor D_0 (in Å^2 /ps) and (b) activation temperature A (in K).

heterogeneous dynamics, which is reflected on the variations of the mean square displacement with two distinct regimes.

The diffusion constants obtained from integrating the velocity autocorrelation functions of centroid or classical hydrogens are represented in Figure 4 as a function of inverse temperature. The results for both bulk and cluster systems are shown in the quantum case, classical results being displayed only for the bulk system in order to improve overall clarity. Error bars are also given for the bulk system, as estimated by the standard deviation between independent calculations from sets of 20 consecutive trajectories to which we added the 5% margin, corresponding to finite Trotter discretization.

The diffusion constants exhibit a linear behavior with inverse temperature when plotted in logarithmic scale, which is represented by the Arrhenius expression of eq 1 but with a size-dependent prefactor $D_0(N)$ and an activation energy $A(N)$. The surprisingly good fit of the simulation results onto the Arrhenius template of eq 1, with regression coefficients above 0.98, suggests that sufficient statistics were gathered in our simulations. These results indicate that diffusion is an activated process in both periodic and finite palladium hydrides. However, they are not as well represented by a $T^{-1/2}\exp(-A/k_BT)$ function, as would be obtained from the Flynn−Stoneham theory,[58] ruling out tunneling as a major contribution within the present quantum model.

The values found for the diffusion constant of bulk systems can be compared with other available results. Li and Wahnström[17] calculated $D(T = 800\ \text{K}) \simeq 1.4-1.5$ Å^2/ ps for the periodic $Pd_{256}H_8$ system, depending on whether non adiabatic effects were neglected or included in the modeling, and $D(T = 1\,000\ \text{K}) \simeq 2.8$ Å^2/ ps. The value reported by these authors at 630 K was found to agree well with available measurements.[59−61] Maeda and co-workers[18] measured $D(T \simeq 823\ \text{K}) \simeq 1.3$ Å^2/ ps, but slightly lower values were experimentally determined by Goltsov et al.[62] and more recently by Powell and Kirkpatrick.[63] All aforementioned studies found the Arrhenius behavior to be well followed, though with different activation energies and prefactors between hydrogen and deuterium. The present RPMD simulations lead to $D(T = 800\ \text{K}) \simeq 1.45$ Å^2/ ps, with the corresponding classical result being $D \simeq 1.30$ Å^2/ ps, in rather satisfactory agreement with published data.

Accounting for quantum delocalization generally enhances diffusion in bulk hydrides but by a small factor close to 10%. We repeated a limited number of simulations for deuterated samples, however, the diffusion appeared too slow for getting reliably converged results at temperatures below 800 K. At 1 000 K, our quantum calculations give a diffusion constant of $D \simeq 2.5$ Å^2 /ps, that is about 11% below the value for hydrogen. This effect is comparable in magnitude to the measured value as reported in the literature.[18,62,63]

Looking now more specifically at clusters, the diffusion constants are much higher than in the bulk system at the same hydrogen concentration, even at the lower common temperature of 500 K. Neglecting quantum vibrational effects, the Arrhenius plots are mainly shifted to slower diffusion by a few percent. More interestingly, the parameters D_0 and A of the Arrhenius form are now found to decrease quite sensitively with cluster size. That hydrogen is more prone to diffusing in clusters than in the bulk has at least two causes. First, diffusion should be easier in the outer, less dense parts of a nanoparticle, which is precisely where the preferred absorption sites lie. Second, the mere presence of hydrogen atoms softens the cluster, and this premelting of the palladium host itself greatly enhances hydrogen motion. This Pd-assisted diffusion mechanism becomes less influential as the cluster size increases because the proportion of subsurface hydrogen atoms decreases concomitantly with an (related) increase in the melting point.

The finite size effects on the diffusion properties can be further quantified by representing the prefactor D_0 and the activation energy A as a function of the inverse cluster radius $R^{-1} \propto N^{-1/3}$. As seen from Figure 5, both D_0 and A display steady decreases with increasing $1/R$ and show some essentially linear variations for clusters containing 128 Pd atoms or more. Some deviations from this linear behavior are found in the smallest species as a manifestation of finite size effects beyond the surface contribution. More generally,

Table II. Parameters of the Liquid Drop Model, eq 9[a]

	classical		quantum	
quantity χ	D_0, Å^2 /ps	A, 10^3 K	D_0, Å^2 /ps	A, 10^3 K
$\chi(\infty)$	25.33	2.285	26.14	2.207
α_S	−93.22	−11.449	−96.18	−7.073
α_E	−363.47	0.603	−346.80	−30.437
α_V	1 510.50	61.413	1 537.21	120.927

[a] For the expansion of the Arrhenius prefactor D_0 and the activation temperature A as a function of $N^{-1/3}$, where N is the cluster size. The results are given for both classical and quantum dynamics.

the variations of D_0 and A with the size N can be approximately described by a liquid drop-like expansion:

$$\chi(N) = \chi(\infty) + \alpha_S N^{-1/3} + \alpha_E N^{-2/3} + \alpha_V N^{-1} + \mathcal{O}(N^{-1}) \quad (9)$$

where χ stands for either D_0 or A and $\chi(\infty)$ is the value of χ at the bulk limit, taken here from the periodic sample. The constant coefficients α_S, α_E, α_V, correspond to the contributions of the surface, edges, and vertices, respectively, relative to the volume. The values of these parameters for classical and quantum dynamics are collected in Table II.

These parameters show comparable values for the classical and quantum systems, except for the second- and third-order contributions to the activation temperature. This is in agreement with Figure 5, where A is higher in the quantum case for the bulk system but lower for the $Pd_{512}H_{16}$ cluster.

The liquid drop extrapolation is especially useful for bridging the gap between the cluster and bulk regimes. The approximately linear rates at which D_0 and A decrease with size will be mostly important for intermediate nanoparticle sizes of experimental relevance, in the 10^1-10^3 nanometers range. At these sizes, our calculations predict that both the prefactor and activation temperature should be attenuated by about 20−30% with respect to the bulk limit.

The diffusion dynamics of hydrogen into Pd clusters can be further studied using the inherent structure approach, where the instantaneous atomic configuration is quenched into the nearest local minimum by standard local optimization. While the energy landscape of classical systems can be exactly partitioned into the basins of attractions of different inherent structures, for quantum systems, the vibrational wave function may extend over multiple basins. However, because both thermal and quantum delocalization are statistical in nature, repeating the quenches captures these combined effects but comparing classical and quantum results allows them to be eventually separated. In the quantum case, we have, thus, assimilated the current configuration as described by the centroids $\bar{\mathbf{R}}$ with weight 1 rather than assigning a weight $1/M$ to each configuration $\mathbf{R}_i$, $1 \le i \le M$. We have performed such a series of quenches for the $Pd_{256}H_8$ bulk or finite systems at 500 K. A number of 200 configurations periodically taken from classical or RPMD trajectories have been locally minimized, and for each resulting minimum, the local coordination of hydrogen atoms has been determined by enumerating the number n_c of Pd atoms distant by less than 2.2 Å. The distributions of coordination numbers for the four situations studied are represented in Figure 6. In fcc palladium, the bimodal distributions indicate that the hydrogens occupy either tetrahedral ($n_c = 4$) or octahedral ($n_c = 6$) sites, the latter being highly favored by quantum effects. The octahedral occupancy of hydrogen for the quantum system is consistent with previous calculations[13,20] and with measurements on deuterated palladium[18,19] and is explained by the lower zero-point energy in these sites.

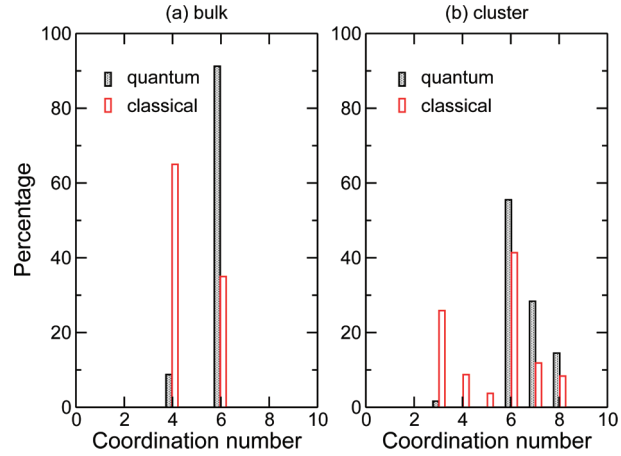

Figure 6. Coordination probability of hydrogen atoms in bulk and finite $Pd_{256}H_8$ systems at 500 K, as obtained from quenching from the centroids or classical positions sampled in equilibrium trajectories.

Hydrogen atoms absorbed in the $Pd_{256}H_8$ cluster exhibit a broader variety of occupancies, covering the $n_c = 3-8$ range. Low-coordinated structures are actually a signature of surface hydrogen atoms, whereas highly coordinated configurations correspond to hydrogens lying near the most dense parts of the icosahedral clusters. Here again, there are marked differences between the inherent structures obtained from both classical and quantum trajectories. The centroids from the quantum dynamics tend to occupy higher coordinated sites but are essentially absent from the surface sites. This may partly result from our removal of trajectories that ended in desorption events, which were more frequent in the quantum case. The broader distribution of coordination numbers is a mere signature of not only the less ordered structure of icosahedral clusters, especially away from the magic numbers of 147 and 309, but also of the surface melted state at this temperature (vide supra). As in the bulk system, we interpret the higher average coordination of hydrogen atoms in the quantum case as another consequence of unfavorable zero-point motion in the low-coordinated sites. However, a direct comparison of the potential and zero-point energies of the inherent structures obtained from the quantum and classical trajectories would not be strictly relevant or even fair because clearly quantum effects drive the system to different parts of the landscape.

IV. Summary and Conclusion

The diffusion of hydrogen in bulk nanoscale metals has found a renewed interest in the context of fuel cell technology. In the present work, we have theoretically studied hydrogen diffusion in palladium nanoparticles paying a particular attention to finite size scaling effects. Using the recently developed ring-polymer molecular dynamics method of

Manolopoulos and co-workers[36] and together with an explicit many-body potential fitted to reproduce energetic and structural properties of bulk palladium hydrides,[13,46,47] we have calculated the diffusion constant of hydrogen in periodic and finite palladium systems. At the low hydrogen concentration of 3%, our calculated diffusion constant for the bulk fcc palladium hydride agrees satisfactorily with previously published experimental results under similar conditions.[18,59−63] In particular, quantum delocalization effects are found to enhance diffusion by a few percents, but no clear signature of tunnel-assisted diffusion was found at the temperature variations of the diffusion constant, which follow some Arrhenius behavior in the range 500−1 000 K.

In Pd clusters containing between 64 and 512 atoms, diffusion is much faster than in the bulk sample. Hydrogen atoms tend to fill the clusters from the outside[9,13] and are found to destabilize or premelt the palladium host, in agreement with previous classical molecular dynamics simulations.[45] The faster diffusion of hydrogen in clusters was interpreted as being due to the less dense outer parts of nanoparticles, together with the mobile character of the corresponding premelted Pd atoms. Even though hydrogen diffuses faster in nanoparticles, the variations of the diffusion constant are still exponential with inverse temperature, with strongly size-dependent prefactor and activation energy. By plotting these Arrhenius parameters as a function of inverse cluster radius, a nearly linear behavior is found between the large clusters containing more than 128 Pd atoms and the bulk limit. Finite-size effects beyond the surface/volume contribution can be represented using a liquid drop expansion up to third order in inverse cluster radius.

While the diffusion constants extracted from quantum and classical trajectories do not overwhelmingly differ from each other, an inherent structure analysis conducted from the centroids positions reveals interesting differences between the two dynamics. When quantum effects are accounted for, hydrogens occupy preferentially octahedral sites in fcc palladium but tetrahedral sites in the classical case.[13,18−20] The much broader variety of occupancies in Pd nanoparticles conveys their less ordered, icosahedral character as well as their partially melted thermodynamical state. However, the same trends noted for the bulk system are found for clusters, namely quantum delocalization favors higher coordinated sites.

Some fundamental aspects touched in this work could be investigated further in the future. Quantifying hydrodynamic effects in the bulk system could be achieved either by estimating the viscosity or, more directly, by performing additional simulations for larger periodic boxes. It would then be interesting to determine whether the corresponding effect, which scales as $1/L \propto N^{-1/3}$ with the number of Pd atoms, is comparable in magnitude to the surface/volume ratio (parameter α_S), which characterizes finite size effects in clusters. Quantum effects on heavier (deuterium) or lighter (muonium) particles could also be envisaged in a more systematic way, not only in the bulk but in clusters as well. Molecular simulation of finite systems would also allow looking into more detailed aspects of the diffusion near the free surfaces by quantifying the extent of diffusion parallel and perpendicular to the surface. It could then be useful to incorporate more robust ways of eliminating the risk of spontaneous desorption after adapting, for instance, the method of Li and co-workers[55] to the RPMD framework.

Finally, it would be useful to apply the ring-polymer molecular dynamics scheme to more complicated systems for which modeling has so far essentially relied on kinetic approximations. Amorphous metals,[28] membranes,[64] and nanoparticle arrays[16] are some examples of possible applications. Ruthenium hydride nanoparticles, for which recent experimental NMR evidence has shown a significant mobility of the hydrogens,[65] also offer promising candidates for testing the present methods in a related context.

Acknowledgment. The authors wish to thank the Pôle Scientifique de Modélisation Numérique (PSMN) for providing the generous computer resources needed.

References

(1) Lewis, F. A. *The Palladium-Hydrogen System*; Academic Press: New York, 1967.

(2) *Hydrogen in Metals I and II*; Alefeld, G., Völkl, J., Eds.; Springer-Verlag: Berlin, Germany, 1978; vols 28 and 29;*Hydrogen in Metals III: Properties and Applications*; Wipf, H., Ed.; Springer-Verlag: Berlin, Germany, 1997.

(3) *Binary Alloy Phase Diagrams*; Massalski, T. B., Ed.; Americal Society for Metals: Metals Park, OH; 1986; vol II.

(4) Graham, T. *Proc. R. Soc.* **1869**, *212*, 17.

(5) Züttel, A. *Mater. Today* **2003**, *6*, 24.

(6) *The Chemical Physics of Solid Surfaces and Heterogeneous Catalysis*; King, D. A., Woodruff, D. P., Eds.; Elsevier: Amsterdam, The Netherlands, 1982.

(7) Huang, S.-Y.; Huang, C.-D.; Chang, B.-T.; Yeh, C.-T. *J. Phys. Chem. B* **2006**, *110*, 21783.

(8) Rather, S.; Zacharia, R.; Hwang, S. W.; Naik, M.; Nahm, K. S. *Chem. Phys. Lett.* **2007**, *438*, 78.

(9) Wolf, R. J.; Lee, M. W.; Ray, J. R. *Phys. Rev. Lett.* **1994**, *73*, 557.

(10) Pundt, A.; Dornheim, M.; Guerdane, M.; Teichler, H.; Ehrenberg, H.; Reetz, M. T.; Jisrawi, N. M. *Eur. Phys. J. D* **2002**, *19*, 333.

(11) Suleiman, M.; Jisrawi, N. M.; Dankert, O.; Reetz, M. T.; Bähtz, C.; Kirchheim, R.; Pundt, A. *J. Alloys Comp.* **2003**, *356−357*, 644.

(12) Pundt, A.; Suleiman, M.; Bähtz, C.; Reetz, M. T.; Kirchheim, R.; Jisrawi, N. M. *Mater. Sci. Eng., B* **2004**, *108*, 19.

(13) Calvo, F.; Carré, A. *Nanotechnology* **2006**, *17*, 1292.

(14) Ingham, B.; Toney, M. F.; Hendy, S. C.; Cox, T.; Fong, D. D.; Eastman, J. A.; Fuoss, P. H.; Stevens, K. J.; Lassesson, A.; Brown, S. A.; Ryan, M. P. *Phys. Rev. B: Condens. Matter* **2008**, *78*, 245408.

(15) Di Vece, M.; Grandjean, D.; Van Bael, M. J.; Romero, C. P.; Wang, X.; Decoster, S.; Vantomme, A.; Lievens, P. *Phys. Rev. Lett.* **2008**, *100*, 236105.

(16) van Lith, J.; Lassesson, A.; Brown, S. A.; Schulze, M.; Partridge, J. G.; Ayesh, A. *Appl. Phys. Lett.* **2007**, *91*, 181910.

(17) Li, Y.; Wahnström, G. *Phys. Rev. Lett.* **1992**, *68*, 3444. *Phys. Rev. B* **1992**, *46*, 14528.

(18) Maeda, T.; Naito, S.; Yamamoto, M.; Mabuchi, M.; Hashino, T. *J. Chem. Soc. Faraday Trans.* **1994**, *90*, 899.

(19) Pitt, M. P.; Gray, E. MacA. *Europhys. Lett.* **2003**, *64*, 344.

(20) Caputo, R.; Alavi, A. *Mol. Phys.* **2003**, *101*, 181.

(21) Kang, B.-S.; Sohn, K.-S. *Physica B* **1995**, *205*, 163.

(22) Kamakoti, P.; Sholl, D. S. *J. Membr. Sci.* **2003**, *225*, 145.

(23) Jewell, L. J.; Davis, B. H. *Appl. Catal., A* **2006**, *310*, 1.

(24) Sundell, P. G.; Wahnström, G. *Phys. Rev. Lett.* **2004**, *92*, 155901.

(25) Dyer, M.; Zhang, C.; Alavi, A. *ChemPhysChem* **2005**, *6*, 1711.

(26) Olsen, R. A.; Kroes, G. J.; Løvvik, O. M.; Baerends, E. J. *J. Chem. Phys.* **1997**, *107*, 10652.

(27) Watson, G. W.; Wells, R. P. K.; Willcock, D. J.; Hitchings, G. J. *J. Phys. Chem. B* **2001**, *105*, 4889.

(28) Hao, S.; Sholl, D. S. *J. Chem. Phys.* **2009**, *130*, 244705.

(29) Gillian, M. J. *J. Phys. C* **1986**, *19*, 6169.

(30) Muranaka, T.; Uehara, K.; Takasu, M.; Hiwatari, Y. *Molec. Sim.* **1994**, *12*, 329.

(31) Gross, A.; Scheffler, M. *Phys. Rev. B: Condens. Matter* **1998**, *57*, 2493.

(32) Busnengo, H. F.; Pijper, E.; Kroes, G. J.; Salin, A. *J. Chem. Phys.* **2003**, *119*, 12553.

(33) Feynman, R. P.; Hibbs, A. R. *Quantum mechanics and path integrals*; McGraw-Hill: New York, 1965.

(34) Chen, B.; Gomez, M. A.; Sehl, M.; Doll, J. D.; Freeman, D. J. *J. Chem. Phys.* **1996**, *21*, 9686.

(35) Forsythe, K. M.; Makri, N. *J. Chem. Phys.* **1998**, *108*, 6819.

(36) Craig, I. R.; Manolopoulos, D. E. *J. Chem. Phys.* **2004**, *121*, 3368.

(37) Cao, J.; Voth, G. A. *J. Chem. Phys.* **1993**, *99*, 10070.

(38) Braams, B. J.; Manolopoulos, D. E. *J. Chem. Phys.* **2006**, *125*, 124105.

(39) Miller, T. F., III; Manolopoulos, D. E. *J. Chem. Phys.* **2005**, *122*, 184503.

(40) Miller, T. F., III; Manolopoulos, D. E. *J. Chem. Phys.* **2005**, *123*, 154504.

(41) Markland, T. E.; Habershon, S.; Manolopoulos, D. E. *J. Chem. Phys.* **2008**, *128*, 194506.

(42) Calvo, F. *J. Comput. Theor. Nanosci.* **2008**, *5*, 331.

(43) Jortner, J. *Z. Phys. D: At., Mol. Clusters* **1992**, *24*, 247.

(44) Wolf, R. J.; Lee, M. W.; Davis, R. C.; Fay, P. J.; Ray, J. R. *Phys. Rev. B: Condens. Matter* **1993**, *48*, 12415.

(45) Grönbeck, H.; Tománek, D.; Kim, S. G.; Rósen, A. *Chem. Phys. Lett.* **1997**, *264*, 39. *Z. Phys. D: At., Mol. Clusters* **1997**, *40*, 469.

(46) Zhong, W.; Li, Y. S.; Tománek, D. *Phys. Rev. B: Condens. Matter* **1991**, *44*, 13053.

(47) Rey, C.; Gallego, L. J.; García-Rodeja, J.; Alonso, J. A.; Iñiguez, M. P. *Phys. Rev. B: Condens. Matter* **1993**, *48*, 8253.

(48) Hone, T. D.; Rossky, P. J.; Voth, G. A. *J. Chem. Phys.* **2006**, *124*, 154103.

(49) Tuckerman, M. E.; Berne, B. J.; Martyna, G. J. *J. Chem. Phys.* **1992**, *97*, 1990.

(50) Pérez, A.; Tuckerman, M. E.; Müser, M. H. *J. Chem. Phys.* **2009**, *130*, 184105.

(51) Witt, A.; Ivanov, S. D.; Shiga, M.; Forbert, H.; Marx, D. *J. Chem. Phys.* **2009**, *130*, 194510.

(52) Dünweg, B.; Kremer, K. *J. Chem. Phys.* **1993**, *99*, 6983.

(53) Yeh, I.-C.; Hummer, G. *J. Phys. Chem. B: Condens. Matter* **2004**, *108*, 15873.

(54) Liu, P.; Harder, E.; Berne, B. J. *J. Phys. Chem. B* **2004**, *108*, 6595.

(55) Li, Y.; Krilov, G.; Berne, B. J. *J. Phys. Chem. B* **2005**, *109*, 463.

(56) Beck, T. L.; Marchioro, T. L., II *J. Chem. Phys.* **1990**, *93*, 1347.

(57) Values much higher than 24 could have been used for *M* if the Pd-H interactions had been additive, in which case the system could be partitioned into classical (Pd) and quantum (H) subsystems.

(58) Flynn, C. P.; Stoneham, A. M. *Phys. Rev. B: Condens. Matter* **1970**, *1*, 3966.

(59) Sköld, K.; Nelin, G. *J. Phys. Chem. Solids* **1967**, *28*, 2369.

(60) Rowe, J. M.; Rush, J. J.; de Graaf, L. A.; Ferguson, G. A. *Phys. Rev. Lett.* **1972**, *29*, 1250.

(61) Carlile, C. J.; Ross, D. K. *Solid State Commun.* **1974**, *15*, 1923.

(62) Goltsov, V. A.; Demin, V. B.; Vykhodets, V. B.; Kagan, G. Ye.; Geld, P. V. *Phys. Metals Metallog.* **1970**, *29*, 195.

(63) Powell, G. L.; Kirkpatrick, J. R. *Phys. Rev. B: Condens. Matter* **1991**, *43*, 6968.

(64) Semidey-Flecha, L.; Sholl, D. S. *J. Chem. Phys.* **2008**, *128*, 144701.

(65) Pery, T.; Pelzer, K.; Buntkowsky, G.; Philippot, K.; Limbach, H.-H.; Chaudret, B. *ChemPhysChem* **2005**, *6*, 605.

CT900554R